A Creep Technique for Monitoring MnS Precipitation in Si Steels

W.P. SUN, W.J. LIU, and J.J. JONAS

A newly developed creep method is described for investigating the kinetics of manganese sulfide precipitation in two Si steels at hot working temperatures. The method was also applied to a Ti steel, in which the precipitation kinetics were previously determined using a stress relaxation technique. Prior to loading, the specimens are solution-treated for half an hour and then immediately cooled to the test temperature. A constant stress is applied to the sample by means of a computerized MTS machine, and the strain is recorded continuously during testing. The resulting creep rate is sensitive to the occurrence of precipitation; thus, the slope of the true strain-log (time) curve decreases immediately after the initiation and increases on the completion of precipitation. The precipitation-time-temperature (PTT) diagrams determined in this way on the three tested steels are of classical C shape. Because higher dislocation densities and internal stress levels are maintained, the present technique is more effective for monitoring the precipitation events occurring in both austenitic and ferritic phases than the previously developed stress relaxation method.

I. INTRODUCTION

THE dissolution and precipitation of second phases play important roles during the processing of steels.[1–4] In order to monitor the progress of precipitation, it is essential to develop reliable techniques which can provide information under the conditions of interest. Although a fairly wide variety of methods, such as electron microscopy,[5–9] chemical or electrochemical extraction,[10–13] and the measurement of electrical resistivity,[14,15] have been employed, the mechanical techniques (in conjunction with electron microscopy) are preferred for several reasons. First, mechanical testing can be performed directly at the temperature at which precipitation takes place, so that the technique is ideally suited to studying precipitation behavior in phases which are unstable at room temperature;[16–19] second, mechanical testing effectively "samples" the entire specimen, whereas a much smaller proportion of each specimen is investigated when electron microscopy alone is employed;[4,16–19] third, the experimental time and effort required to determine PTT relationships are much less than required for the other methods.[17–20]

Among the mechanical methods, the stress relaxation technique is of particular interest because of its high sensitivity, small sampling error, and experimental ease. However, this method has so far only been employed for following the progress of precipitation in austenite.[4,19,20] Indeed, initial attempts to use it to detect sulfide precipitation in ferrite have been unsuccessful.[20] Thus, efforts have been made to find an alternative mechanical technique suitable for determining precipitation kinetics in ferrite as well as in austenite.

W.P. SUN, Graduate Student, and J.J. JONAS, CSIRA-NSERC Professor of Steel Processing, are with the Department of Metallurgical Engineering, McGill University, Montreal, PQ, Canada H3A 2A7. W.J. LIU, formerly with the Department of Metallurgical Engineering, McGill University, is Research Associate with the Centre for Metallurgical Process Engineering, University of British Columbia, Vancouver, BC, Canada V6T 1W5.

Manuscript submitted May 1, 1989.

The method of creep testing described below was developed in response to this need. In order to improve the creep resistance of materials, many studies have dealt with the effects of second-phase particles on the creep properties of metals.[21–25] Despite the increasingly good understanding of the interaction between precipitation and strength, little work has been carried out to date on the use of creep data for the measurement of precipitation kinetics. In the present paper, a mechanical technique based on the analysis of creep behavior is introduced. The results obtained with regard to precipitation in both ferritic and austenitic steels are presented, and the sensitivity of the technique is compared to that of the stress relaxation method developed earlier.[19]

II. EXPERIMENTAL MATERIALS AND TECHNIQUE

A. *Material Preparation*

The kinetics of MnS precipitation in two electrical steels, which remain ferritic at all temperatures up to the melting point, and that of Ti(CN) in a microalloyed austenite were investigated at high temperatures. The experimental materials were provided by Dofasco Inc., Hamilton, Ont. and the Metals Technology Laboratories of the Department of Energy, Mines, and Resources, Ottawa in the form of hot-rolled plates. Their chemical compositions are listed in Table I. The concentrations of Mn and S were 0.07 and 0.021 wt pct in Si steel A and 0.125 and 0.015 in Si steel B. The Si level in both these steels was approximately 3 pct. The Ti steel, which was used in a previous study,[4,19] had a Ti level of 0.25 pct, with a base composition typical of microalloyed plate steels.

Compression samples 11.9 mm in height and 7.9 mm in diameter were machined from the as-received plates, with their longitudinal axes parallel to the rolling direction. Concentric flat-bottomed grooves 0.15-mm deep, 0.36-mm wide, and spaced at 0.46-mm intervals were

Table I. Chemical Composition in Weight Percent of the Steels Tested

Steel	C	Si	Ti	Al	Mn	N	P	S
Si Steel A	0.025	3.13	—	0.003	0.070	0.005	0.006	0.021
Si Steel B	0.029	3.00	—	0.007	0.125	0.004	0.003	0.015
Ti Steel	0.050	0.27	0.25	0.01	1.43	0.007	0.005	0.010

cut into the end faces to accumulate the glass lubricants applied to the sample/anvil interface during testing.[26]

B. *Experimental Procedure*

The experiments were carried out on a computerized mechanical testing system set up for hot compression testing. This system consists of an MTS testing machine, a high-temperature vacuum furnace, and a helium quenching device. The thermomechanical treatment schedules are presented in Figure 1. Prior to the application of the load, the samples were heat-treated for half an hour at 1300 °C for the electrical steels and 1260 °C for the Ti steel. This treatment led to the complete dissolution of the sulfide in the Si steels and of the C-rich carbonitride in the Ti steel. The dissolution temperatures employed in this schedule are about 50 °C higher than the equilibrium solution temperatures of MnS and TiC calculated from the solubility products reported in the literature.[27-31] After such treatment, each specimen was immediately cooled to the test temperature at a mean rate of about 2 °C/s by shutting off the power supply of the furnace. The test temperatures ranged from 800 °C to 1100 °C for the Si steels and from 900 °C to 1100 °C for the Ti steel. On attaining the test temperature, a holding interval of 1 minute was employed to permit the specimen temperature to become uniform. Then, a constant stress was applied to the specimen for up to 1 hour, and the strain was continuously recorded. During each creep test, the temperature was held constant to within ±1 °C.

C. *Determination of Applied Stress for Experiment*

It is important to note that the applied stress must be carefully selected if precipitation is to be detected by the creep method. On a trial basis, it was found that the creep rate is sensitive to the occurrence of precipitation when the applied stress corresponds to the steady-state stress of the steel hot-compressed at a strain rate of about 10^{-4} s^{-1}. Thus, preliminary tests were first carried out to determine the flow curves of the steels at a strain rate of 10^{-4} s^{-1} directly at each temperature of interest without employing any prior solution heat treatment. A family of true stress-true strain curves established in this way is shown in Figure 2 for one of the 3 pct Si steels. Here, the steady-state stresses in the region in which the net rate of work hardening is approximately zero are readily seen. The values defined in this way were employed as applied stresses for each testing temperature in question.

D. *Creep Test*

Computer monitoring and data acquisition for the creep tests were supervised by means of a program written in MTS BASIC/RT-11. Since cooling from the solution temperature is involved in the present method, the tooling of the machine contracts as the temperature decreases. Hence, the raw creep data contain a contribution from the temperature-induced contraction, which can obviously interfere with the determination of the precipitation kinetics during the first few hundred seconds of deformation. To remove the length change contribution from the raw creep data, the ram displacement due to the temperature decrease *vs* time relationship was first determined using the technique developed by Liu and Jonas[19] for stress relaxation testing. For each test temperature, the measured displacements were stored as length contractions of the tooling. These data were employed for correction of the raw creep data by subtracting the tool length decrease from the creep strain. This

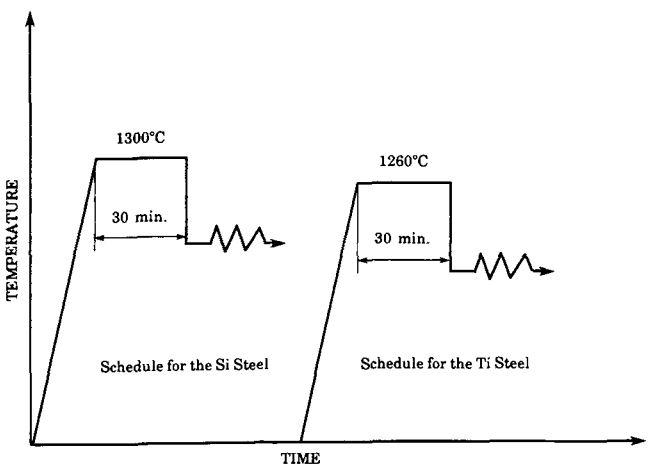

Fig. 1—Thermomechanical treatment schedules.

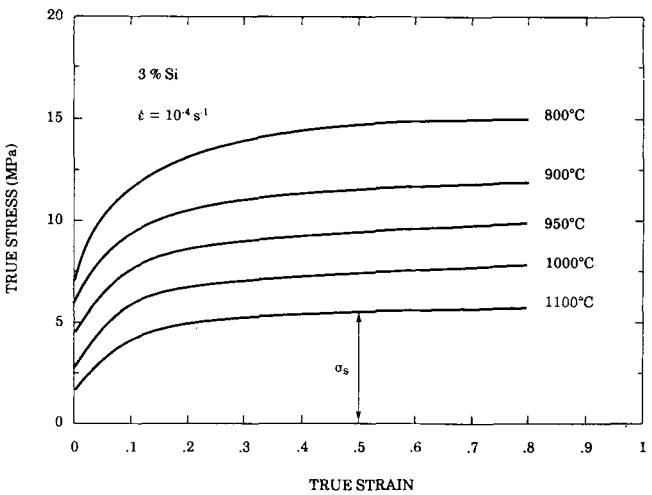

Fig. 2—Typical flow curves obtained at a strain rate of 10^{-4} s^{-1} for the 3 pct Si steel.

correction routine was incorporated into the program, and only the corrected creep data are reported below.

E. *Electron Microscopy*

The freshly precipitated particles and their compositions were studied with the help of extraction replicas. The helium-quenched samples were first cut parallel to the compression direction with a low-speed diamond saw operated with a coolant. Next, the resulting pieces were mounted in bakelite, and the sectioned surfaces were ground using silicon carbide papers. Then, they were prepared by mechanical polishing with 6-μm diamond paste and 0.3-μm alumina in sequence for the Ti steel and by electrolytic polishing in a 50-50 solution by volume of 30 pct H_2O_2-85 pct H_3PO_4 for the Si steels. The polished samples of Ti steel were lightly etched in 3 pct HNO_3-97 pct C_2H_5OH and those of the Si steels in 1 pct HNO_3-99 pct C_2H_5OH. Subsequently, the polished-and-etched surfaces were coated with a carbon layer about 20-nm thick in a vacuum evaporator; the carbon layer was cut into 3 × 3 mm squares with a scalpel blade, and then released and placed on transmission electron microscope copper grids. Finally, the precipitates in the carbon replicas were examined in a JEOL-100 CX scanning transmission electron microscope fitted with a PGT system IV energy dispersive X-ray spectrometer (EDS) for the chemical analysis of individual particles.

III. EXPERIMENTAL RESULTS

A. *Conventional Creep Testing*

The basic shape of the creep curve for electrical steel A is illustrated in Figure 3(a). In this case, the thermomechanical treatment shown in the inset was carried out. The test was performed at 900 °C after half an hour of aging at the same temperature so that no precipitation took place during deformation in this case. During such tests, the steel was stressed at 900 °C for as long as 1 hour. Figure 3(a) shows that after a primary stage of creep lasting for a few hundred seconds, the creep rate remains approximately constant during the secondary stage of creep until the end of the test. When the data are plotted in terms of strain *vs* log(time), as in Figure 3(b), it is evident that the true strain increases smoothly as log(time) increases, and no plateau is present on this curve.

B. *Experimental Curves*

Some typical creep data obtained by the present technique on electrical steel A at 900 °C are shown in Figure 4. From this figure, it can be seen that the slope of the creep strain with respect to the log(time) curve first increases during loading and then decreases after about 15 seconds of creep. The slope begins to increase again at about 420 seconds. The points on the curve at which the plateau begins and ends, as will be demonstrated in more detail below, can be attributed to the occurrence of precipitation during creep. Identifying these two points as P_s (precipitation start time) and P_f (precipitation finish time), these can be evaluated more precisely in terms of

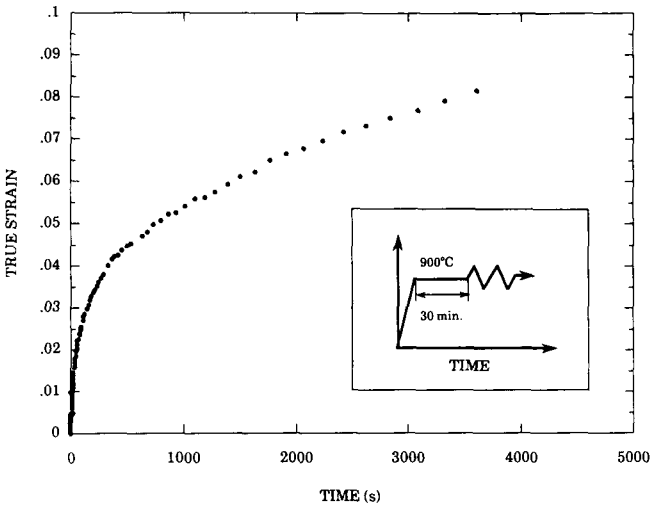

(*a*)

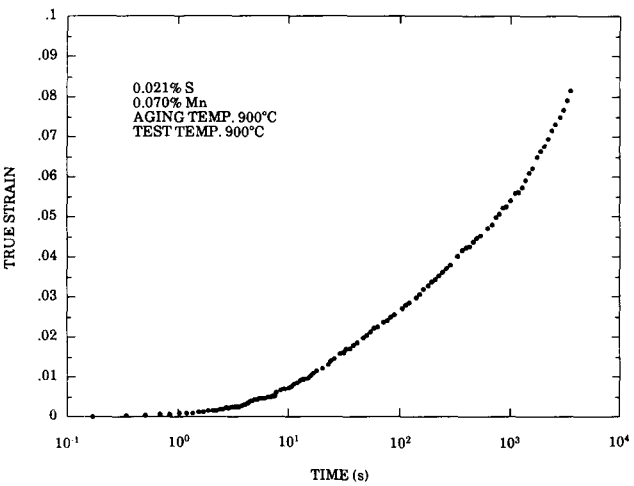

(*b*)

Fig. 3—Typical true strain curve obtained during conventional creep testing for Si steel A at 900 °C plotted against (*a*) time and (*b*) log(time).

the second derivatives of the strain with respect to log(time). The latter change from positive to negative at P_s and become positive again at P_f. Thus, P_s and P_f can be defined by the following equations:

$$\left.\frac{\partial^2(\varepsilon)}{\partial(\ln t)^2}\right|_{t=P_s} = 0, \quad \text{and} \quad \left.\frac{\partial^3(\varepsilon)}{\partial(\ln t)^3}\right|_{t=P_s} < 0 \qquad [1]$$

$$\left.\frac{\partial^2(\varepsilon)}{\partial(\ln t)^2}\right|_{t=P_f} = 0, \quad \text{and} \quad \left.\frac{\partial^3(\varepsilon)}{\partial(\ln t)^3}\right|_{t=P_f} > 0 \qquad [2]$$

where ε is the creep strain, and t is the creep time.

True strain-log(time) curves for the three experimental steels are presented in Figure 5. The precipitation start P_s and finish P_f times identified in this way are indicated by arrows in these diagrams. From the curves, it is apparent that (1) the higher the testing temperature, the larger the creep strain in a given time, and (2) the strain plateaus become more marked as the testing temperature is decreased.

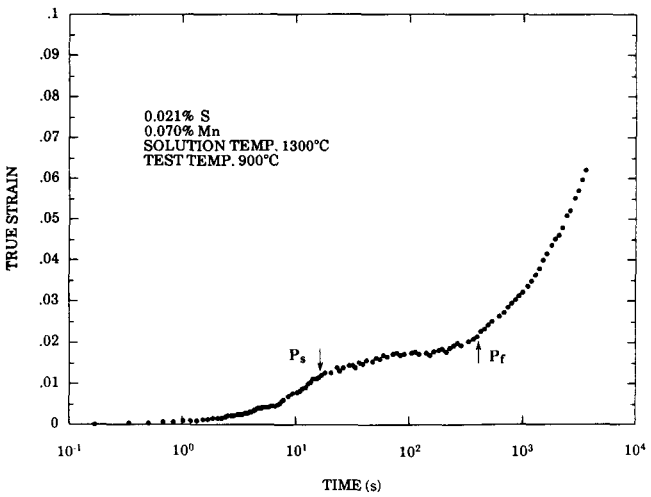

Fig. 4—Typical true strain-log(time) curve obtained by the present creep technique for Si steel A at 900 °C.

C. *Morphology and Composition of the Precipitates Formed during Creep*

As shown above, an alloy in which a second phase is precipitated displays departures from conventional creep behavior. Direct structural evidence for this phenomenon was obtained by means of electron microscopy. The quenching schedule employed for this purpose is shown in the upper left-hand corner of Figure 6. Samples (*b*) and (*d*) were helium-quenched close to the P_s and P_f times defined above. Sample (*a*) was quenched prior to P_s, sample (*c*) between P_s and P_f, and sample (*e*) at the end of the test.

In Figure 6, electron micrographs are presented for Si steel A undergoing creep at 900 °C. No precipitates were found in the sample which was quenched prior to P_s (Figure 6(a)), while very small precipitates ranging from about 2 to 15 nm were occasionally observed after 15 seconds of creep (Figure 6(b)). This supports the interpretation that it is the formation of these precipitates that arrests the creep rate. As the creep time was increased to 60 seconds, the density of precipitates increased significantly, and the particle size distribution broadened to cover the range from 2 to 40 nm, as illustrated in Figure 6(c). As the creep time was further increased, the mean size of the precipitates increased continuously, but the density of the particles decreased, as shown for 420 seconds in Figure 6(d). This indicates that P_f is associated with the start of the dissolution of small particles and the coarsening of the large precipitates, as in the case of stress relaxation.[19,32] The significant particle coarsening taking place after P_f is illustrated in Figure 6(e).

The freshly precipitated particles were investigated by examining their X-ray spectra. A typical result is presented in Figure 7, which reveals the strong Mn and S peaks associated with most of the particles formed in the Si steels. Thus, it can be concluded that manganese sulfide precipitates are responsible for the hardening effect observed during the creep of the two electrical steels tested.

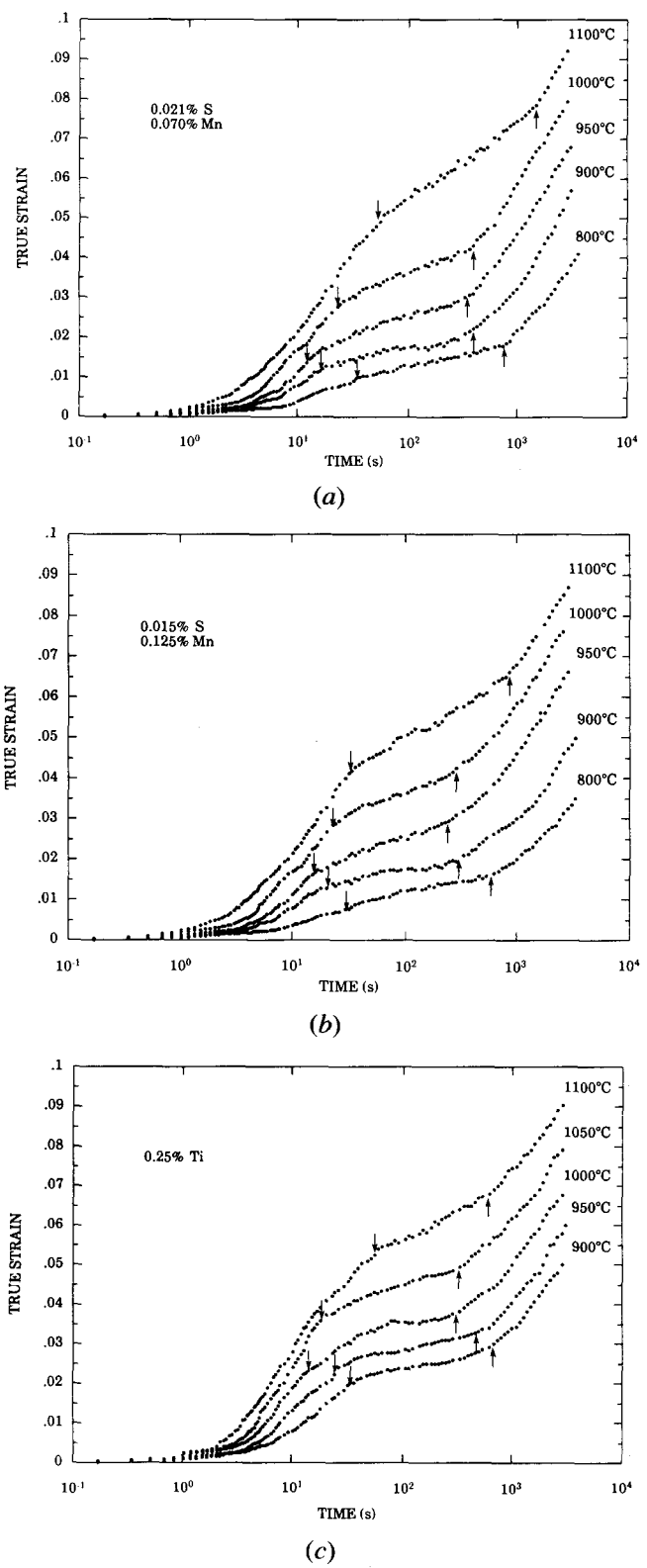

Fig. 5—Creep strain *vs* log(time) curves for the (*a*) Si A, (*b*) Si B, and (*c*) Ti steels.

D. *PTT Diagrams*

The P_s and P_f times determined by the present method for the two electrical steels are presented in the form of PTT diagrams in Figure 8. It is apparent from this figure that the curves for MnS precipitation in ferrite are of the

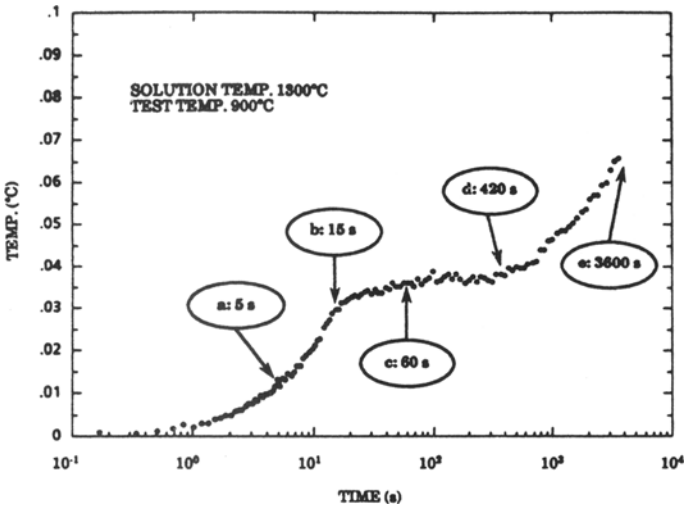

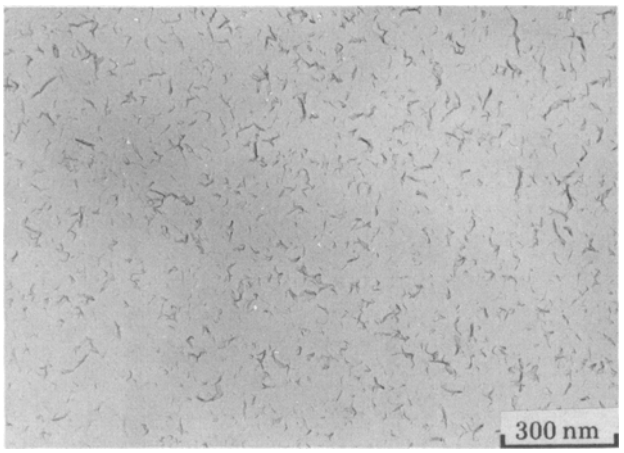

(*a*)

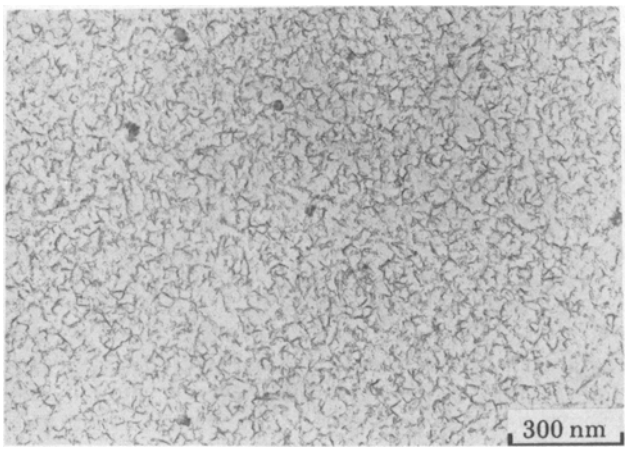

(*b*)

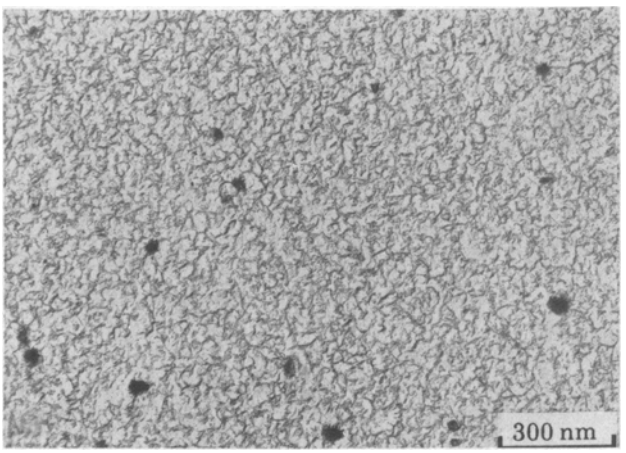

(*c*)

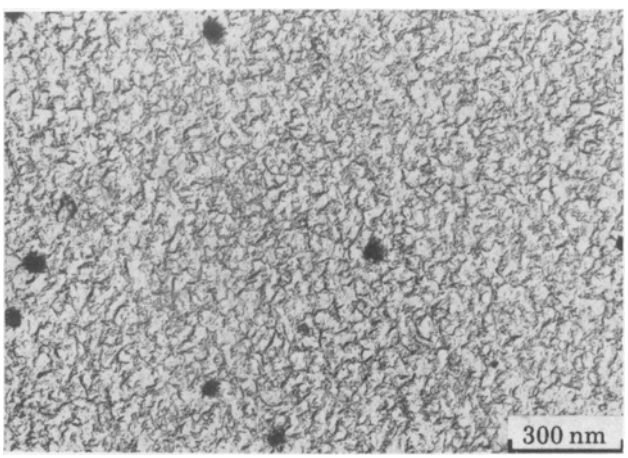

(*d*)

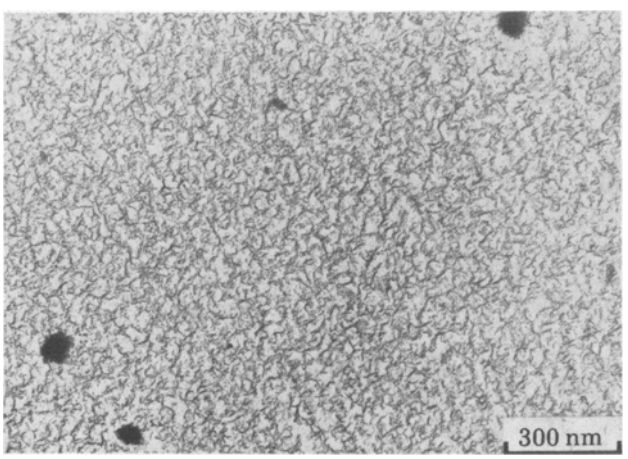

(*e*)

Fig. 6—Carbon extraction replicas showing the progress of MnS precipitation in samples of Si steel A undergoing creep at 900 °C: (*a*) 5 s, (*b*) 15 s, (*c*) 60 s, (*d*) 420 s, and (*e*) 3600 s.

classical C shape, with the nose at a minimum time of about 12 seconds at 950 °C for the 0.021 pct S Si steel and at 14 seconds and 950 °C for the 0.015 pct S steel. Comparison between the two curves reveals that there is little difference in the precipitation start time between the two materials. The similarity of the P_s times suggests that the driving forces for MnS nucleation in the two steels are nearly identical. By contrast, the P_f times for the 0.021 pct S Si steel are significantly longer than for the 0.015 pct S Si steel. Note that P_f is mainly determined by the growth rate of the MnS particles once the nucleation rate has been established. This growth rate is

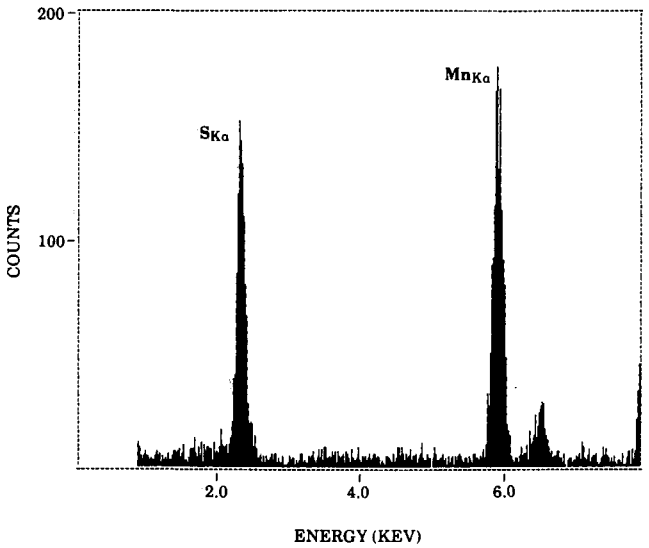

Fig. 7—Typical X-ray spectrum of MnS particles displaying strong Mn and S peaks.

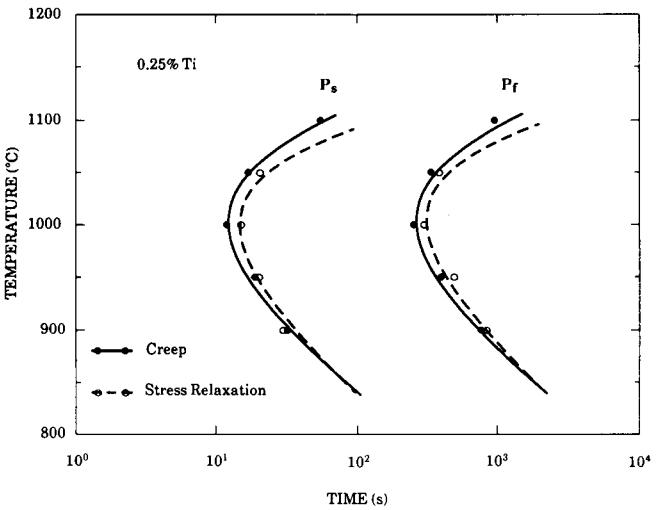

Fig. 9—Comparison of the PTT curves obtained for the 0.25 pct Ti steel by the present method with those determined by the stress relaxation technique.

controlled by the diffusion of Mn in the present alloy system, since the diffusivity of Mn is about an order of magnitude slower than that of S in iron.[33] As a result, the higher Mn level (0.125 pct) in the 0.015 pct S steel leads to a faster MnS growth rate and, therefore, to shorter P_f times.

The PTT curve for the Ti-bearing steel is shown in Figure 9, together with the results obtained from the earlier stress relaxation technique.[19] It is important to note that experimental points were readily obtained by the creep method at 1100 °C, conditions under which the stress relaxation test is too insensitive to detect changes in the state of precipitation. The reasons for the higher sensitivity of the creep technique are of considerable practical interest and will be discussed in more detail below.

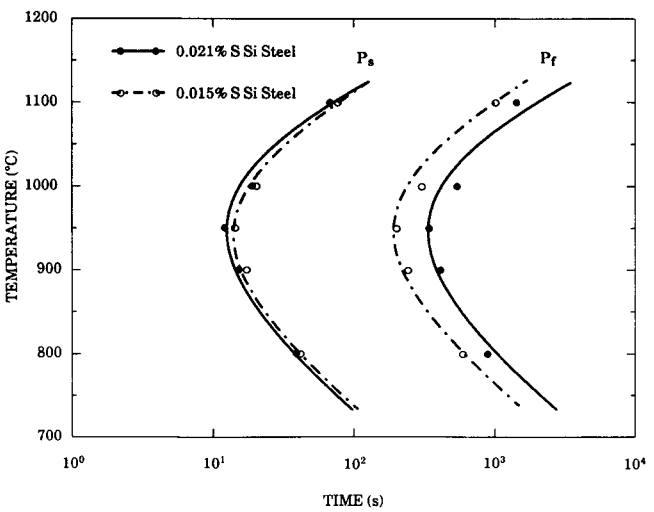

Fig. 8—PTT curves for the two S-bearing Si steels determined by the present technique.

IV. DISCUSSION

A. *Applicability of the Present Technique for Following Precipitation in Ferrite*

As mentioned at the beginning of this article, attempts to use the stress relaxation method to detect MnS precipitation in Si steels have been unsuccessful to date. Therefore, it is relevant to explore why the creep technique is more suitable than the stress relaxation method for investigating precipitation behavior in ferritic steels. It should first be recognized that during stress relaxation, the sum of the elastic and creep components of the strain (ε_e and ε_c, respectively) are equal to the initial elastic strain, ε_{e0}. Thus, neglecting anelastic effects,

$$\varepsilon_{e0} = \varepsilon_e + \varepsilon_c \qquad [3]$$

Differentiating,

$$\left(\frac{1}{E^*}\right)\frac{d\sigma_a}{dt} + \dot{\varepsilon}_c = 0 \qquad [4]$$

where σ_a is the applied stress during stress relaxation, and E^* is the combined elastic modulus defined in terms of the elastic moduli of the specimen (E) and testing machine (E°) as follows:

$$\frac{1}{E^*} = \frac{1}{E} + \frac{1}{E^\circ} \qquad [5]$$

The analysis of stress relaxation phenomena in physical terms is not simple, but a first approximation can be obtained by relating the creep rate to the effective stress σ^* by a power law:[34]

$$\dot{\varepsilon}_c = B^*\sigma^{*n} \qquad [6]$$

Substituting the above into Eq. [4],

$$\left(\frac{1}{E^*}\right)\frac{d\sigma_a}{dt} = -B^*\sigma^{*n} \qquad [7]$$

As

$$\sigma_a = \sigma^* + \sigma_i \quad [8]$$

where σ_i is the internal stress of the specimen during stress relaxation, Eq. [7] can be transformed into

$$\left(\frac{1}{E^*}\right)\frac{d(\sigma^* + \sigma_i)}{dt} = -B^*\sigma^{*n} \quad [9]$$

By assuming that the internal stress, σ_i, is constant during stress relaxation and then integrating the above relation, the effective stress at any time, t, can be expressed as

$$\sigma^* = \frac{\sigma_0^*}{[1 + B^*E^*(n-1)\sigma_0^{*n-1}t]^{1/n-1}} \quad [10]$$

where σ_0^* is the initial value of the effective stress.

The quantitative estimation of σ_i and σ^* requires some input regarding the initial conditions. For this purpose, we first assume that

$$\sigma_{i0} \simeq 0.5\sigma_{a0} \quad [11]$$

where σ_{i0} and σ_{a0} are the initial values of the internal and applied stresses, respectively. At the very beginning of stress relaxation ($t = 0$), we therefore have

$$\sigma_0^* = \sigma_{a0} - \sigma_{i0} = 0.5\sigma_{a0} \quad [12]$$

Employing the present experimental observations for σ_{a0}, the data for E° reported by Liu[4] and for E, B^*, and n by Frost and Ashby[35] in the above equations, the applied stresses for the 3 pct Si and 0.25 pct Ti steels were calculated for stress relaxation after a 5 pct prestrain at 900 °C. These are presented together with the experimental results in Figure 10.

After comparing the predictions for the Ti steel with the experimental curves obtained in the previous study,[19,20] it is evident that the assumption that the internal stress σ_i remains approximately constant as stress relaxation proceeds is consistent with the observations. For Si steel A, however, there is a large difference between the calculated and measured values of the applied stress. Hence, the assumption that the internal stress σ_i is constant and equal to about half of σ_{a0} during stress relaxation is seen to be untenable for ferritic steels. Such steels, like most bcc metals, have higher stacking fault energies than when in the austenite condition, so that after straining is interrupted, more recovery is expected during the course of stress relaxation.

The effects of such recovery can be readily evaluated by making some assumptions about the kinetics of the process. For example, the recovery of internal stress can be considered to follow zero-order kinetics, so that

$$\sigma_i = \sigma_{i0} - k_0 t \quad [13]$$

Here, k_0 is a zero-order rate constant and is given by the decrement of internal stress per unit time. Alternatively, if the recovery of internal stress follows first-order kinetics, σ_i takes the form

$$\sigma_i = \sigma_{i0}\exp(-k_1 t) \quad [14]$$

where k_1 is the first-order rate constant. The substitution of Eqs. [13] and [14] into Eq. [9] leads to

$$\frac{d\sigma^*}{dt} - k_0 = -B^*E^*\sigma^{*n} \quad [15]$$

and

$$\frac{d\sigma^*}{dt} - k_1\sigma_{i0}\exp(-k_1 t) = -B^*E^*\sigma^{*n} \quad [16]$$

respectively.

The above equations were solved by the Runge-Kutta method. The results obtained were substituted into Eq. [8], leading to the family of applied stress curves presented in Figure 11. It is evident that the predicted values match the experimental results when the recovery of internal stress is described by the first-order kinetics model (but not the zero-order model). Thus, it appears that the recovery of internal stress is responsible for the rapid decrease in applied stress in the first second in the Si steel.

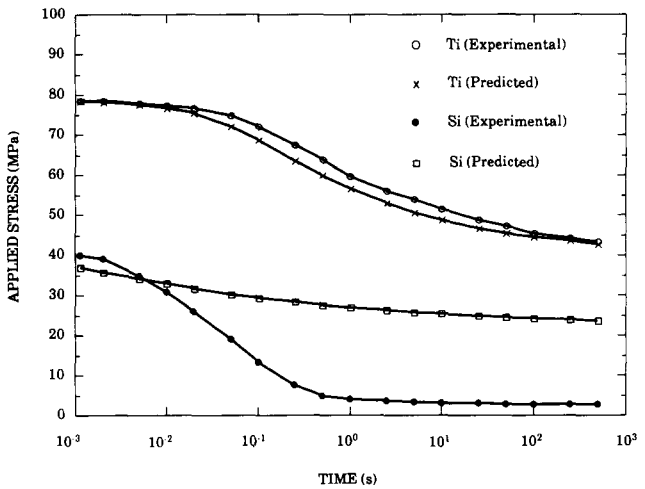

Fig. 10—Measured and predicted applied stresses for the relaxation of the 3 pct Si and 0.25 pct Ti steels after a 5 pct prestrain at 900 °C.

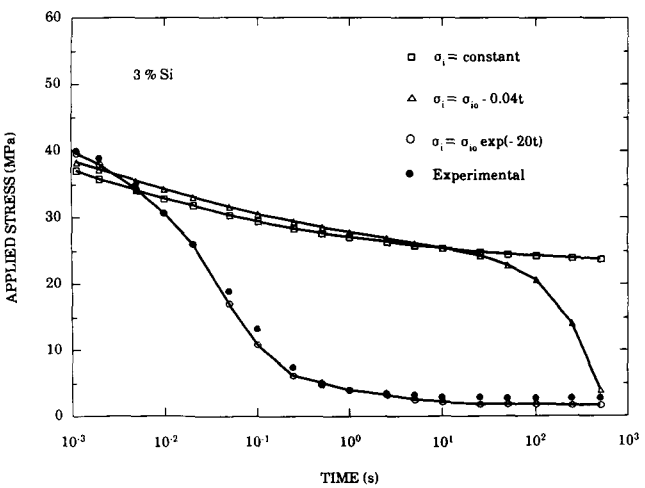

Fig. 11—Applied stresses measured and predicted by various models for the relaxation of the 3 pct Si steel after a 5 pct prestrain at 900 °C.

Furthermore, the softening process develops so quickly that the internal stress nearly disappears well before the initiation of MnS precipitation (15 seconds at this temperature). Such an exponential decay of internal stress supports the view that dislocations in ferritic steels are readily annihilated during stress relaxation. Bearing in mind that the detection of precipitation by mechanical methods relies on the interaction between precipitates and dislocations,[19] it is clear that the rapid disappearance of dislocations in ferritic steels makes it difficult to use the stress relaxation method in these materials. By contrast, the present creep technique, by holding the stress constant during testing, maintains the dislocation density at a high enough level that the progress of precipitation can be monitored for as long as 1 hour in ferritic steels, as well as in austenitic steels at elevated temperatures.

B. *Comparison of the Sensitivity of the Creep Technique with that of the Stress Relaxation Method*

The PTT diagrams obtained in the present work for the 0.25 pct Ti steel were compared with those determined by the stress relaxation method[19] in Figure 9. It is apparent from this figure that above 950 °C, there is a slight shift to the left in the P_s curve determined by the present technique. Furthermore, the stress relaxation method was not sensitive enough to detect the start and finish of precipitation at 1100 °C, whereas the creep technique led to the ready definition of both the P_s and P_f times at the latter temperature. The explanation of these phenomena is the same as why the creep method is able to handle ferritic steels. After deformation at temperatures as high as 1100 °C, even austenitic steels undergo significant static recovery, during which most of the dislocations within the material are readily annihilated. This inherent shortage of dislocations seems to be a shortcoming of the stress relaxation method. By contrast, dislocations are continuously being generated and recovered during creep. As a result, the creep technique can be employed at higher temperatures than the stress relaxation method, even in austenitic steels.

V. CONCLUSIONS

A new mechanical method has been developed for detecting precipitation start and finish times in both ferrite and austenite at hot working temperatures. The following conclusions can be drawn from the results of this study:

1. During creep testing, the creep rate is sensitive to the occurrence of precipitation; thus, the slope of the creep strain-log(time) curve decreases markedly after the initiation of precipitation and increases on the completion of precipitation. Accordingly, the left- and right-hand ends of the plateaus on these curves can be identified as the precipitation start and finish times, respectively.
2. The PTT diagrams determined by the technique described here are generally C-shaped. For both Si steels tested, the nose temperature is about 950 °C, while the nose time is 12 seconds for the one containing 0.021 pct S and 0.070 pct Mn and 14 seconds for the one with 0.015 pct S and 0.125 pct Mn. Although there is little difference in precipitation start time between the two materials, the P_f times in the former are considerably longer than in the latter.
3. Recovery rates during stress relaxation obey first-order kinetics in the present ferritic steels and are much higher than in microalloyed steels tested in the austenite range. The high recovery rates rapidly reduce the dislocation density to levels which are too low for the determination of P_s and P_f times by stress relaxation. By contrast, the present creep method, by maintaining the dislocation density at an appropriate level, is capable of detecting the beginning and end of precipitation in these materials.
4. Comparison between the present technique and the stress relaxation method developed earlier shows clearly that the former is more sensitive than the latter when both are employed at high temperatures in the austenite range.

ACKNOWLEDGMENTS

The authors are indebted to A. Pether and P. Nestico of Dofasco Inc., Hamilton, Ont. for supplying the experimental alloys. They thank Drs. X.L. He and S. Yue for their useful comments. The financial support received from the Natural Sciences and Engineering Research Council of Canada, the Canadian Steel Industry Research Association (CSIRA), the Ministry of Education of Quebec (FCAR program), and Dofasco Inc. is acknowledged with gratitude.

REFERENCES

1. X. Sun, Z. He, Y. Chen, M. Ma, and Z. Liu: *Acta Metall. Sin.*, 1985, vol. 21, pp. B17-23.
2. R.W.K. Honeycombe: *HSLA Steels: Metallurgy and Applications*, J.M. Gray, T. Ko, S. Zhang, B. Wu, and X. Xie, eds., ASM, Beijing, People's Republic of China, 1987, pp. 243-50.
3. W.E. Voice and R.G. Faulkner: *Metall. Trans. A*, 1985, vol. 16A, pp. 511-20.
4. W.J. Liu: Ph.D. Thesis, McGill University, Montreal, PQ, Canada, 1987.
5. G. Fitzsimons, K. Tiitto, R. Fix, and A.J. DeArdo: *Metall. Trans. A*, 1984, vol. 15A, pp. 241-43.
6. M. Koizumi, T. Kikuti, and S. Bandô: *Tetsu-to-Hagané*, 1980, vol. 66, pp. 1123-32.
7. S.S. Hansen, J.B. Vander Sande, and M. Cohen: *Metall. Trans. A*, 1980, vol. 11A, pp. 387-402.
8. S. Yamamoto, C. Ouchi, and T. Osuka: *Thermomechanical Processing of Microalloyed Austenite*, P.J. Wray and A.J. DeArdo, eds., AIME, Warrendale, PA, 1982, pp. 613-39.
9. Y.Z. Chen, D. Ma, M. Ge, and E.S. Wang: *Acta Metall. Sin.*, 1978, vol. 14, pp. 33-39.
10. A.T. Davenport, R.E. Miner, and R.A. Kot: *The Hot Deformation of Austenite*, J.B. Ballance, ed., AIME, New York, NY, 1977, pp. 186-203.
11. T.M. Hoogendoorn and M.H. Spanraft: *Microalloying '75*, M. Korchynsky, ed., Union Carbide Corp., New York, NY, 1977, pp. 75-85.
12. H. Watanabe, Y.E. Smith, and R.D. Pehlke: *The Hot Deformation of Austenite*, J.B. Ballance, ed., AIME, New York, NY, 1977, pp. 186-203.
13. K. Iwayama and T. Haratani: *J. Magn. Magn. Mater.*, 1980, vol. 19, pp. 15-17.
14. R. Simoneau, G. Begin, and A.H. Marquis: *Met. Sci.*, 1978, vol. 12, pp. 381-86.
15. S. Fujikawa, Y. Izeki, and K. Hirana: *Scripta Metall.*, 1986, vol. 20, pp. 1275-80.

16. R.K. Amin, G. Butterworth, and F.B. Pickering: *Hot Working and Forming Processing*, C.M. Sellars and G.L. Davies, eds., Sheffield, England, 1980, pp. 27-31.
17. I. Weiss and J.J. Jonas: *Metall. Trans. A*, 1979, vol. 10A, pp. 831-40.
18. J.J. Jonas and I. Weiss: *Met. Sci.*, 1979, vol. 13, pp. 238-45.
19. W.J. Liu and J.J. Jonas: *Metall. Trans. A*, 1988, vol. 19A, pp. 1403-13.
20. W.P. Sun: Ph.D. Thesis, McGill University, Montreal, PQ, Canada, 1989.
21. H.J. Grabke: *Steel Res.*, 1987, vol. 58, pp. 477-82.
22. M. Schumacher and G. Sauthoff: *Z. Metallkd.*, 1987, vol. 78, pp. 582-89.
23. M. Takeyama, K. Kawasaki, T. Matsuo, and R. Tanaka: *Tetsu-to-Hagané*, 1986, vol. 72, pp. 1605-12.
24. J.M. Adamson and J.W. Martin: *Creep Strength in Steel and High-Temperature Alloys*, Iron Steel Institute, University of Sheffield, Sheffield, England, 1972, pp. 99-105.
25. I. Jung and G. Sauthoff: *Creep and Fracture of Engineering Materials and Structures*, Institute of Metals, Swansea, UK, 1987, pp. 250-70.
26. M.J. Luton: Ph.D. Thesis, McGill University, Montreal, PQ, Canada, 1971.
27. N.G. Ainslie and A.V. Seybolt: *J. Iron Steel Inst.*, 1960, vol. 194, pp. 341-50.
28. H.E. Grenoble: *J. Appl. Phys.*, 1967, vol. 38, pp. 1083-86.
29. H.A. Wriedt and Hsun Hu: *Metall. Trans. A*, 1976, vol. 7A, pp. 711-18.
30. E.F. Petrova, A.I. Rogov, V.G. Borisenko, A.G. Petrenko, A.A. Kononov, and L.A. Shvartsman: *Russ. Metall.*, 1976, pp. 117-22.
31. K.J. Irvine, F.B. Pickering, and T. Gladman: *J. Iron Steel Inst.*, 1967, vol. 205, pp. 161-82.
32. W.J. Liu and J.J. Jonas: *Metall. Trans. A*, 1988, vol. 19A, pp. 1415-24.
33. R.C. Weast and M.J. Astle: *Handbook of Chemistry and Physics*, 62nd ed., CRC Press Inc., Boca Raton, Florida, 1982, pp. F54-59.
34. I. LeMay: *Principles of Mechanical Metallurgy*, Elsevier North-Holland Inc., New York, NY, 1981, pp. 337-58.
35. H.J. Frost and M.F. Ashby: *Deformation-Mechanism Maps*, Pergamon Press, Oxford, 1982, pp. 60-70.